

# A Miniatured Specimen Technique for Fracture Toughness ( $J_{IC}$ ) Measurement

XINGYUAN MAO\*, TETSUO SHOJI\*\* and HIDEAKI TAKAHASHI\*\*

\*Nuclear Reactor Laboratory, Massachusetts Institute of Technology, Cambridge, MA 02139, USA

\*\*Research Institute for Strength and Fracture of Materials, Tohoku University, Sendai, Japan

## Abstract

The effect of specimen thickness on fracture toughness has been investigated with compact tension specimens. HT-9 and A533B steel specimens with thickness of 25(1CT), 10(0.4CT), 3 and 0.5(0.2CT) mm were tested. Some of them did not satisfy the ASTM size requirement for valid  $J_{IC}$ (E813). The through-thickness distribution of the plastic energy dissipation within the intense strain region at the crack tip was measured by using a recrystallization-etch technique. Fractographic examinations on stretch zone width and fracture modes along the thickness of specimen were performed by scanning electron microscope (SEM). A new  $J_{IC}$  evaluation procedure for invalid specimen size is proposed using rigid plastic analysis and shear fracture measurement. Then the predicted  $J_{IC}$  values are compared with the  $J_{IC}$  values obtained from valid specimen size. This miniaturized specimen technique may be applicable to post-irradiation fracture toughness testing.

## KEYWORDS:

fracture toughness, valid size, thickness effects recrystallization-etch method, flat and shear fracture stretched zone, plane stress and plane strain condition

## 1. Introduction

The nature of both the design and alloy development approaches for large system, and nuclear system in particular, necessitates the development and application of a small specimen technique for fracture toughness evaluation. The size limitation in irradiation volume for material irradiation test is so small that it can not meet ASTM size requirements for valid fracture toughness  $J_{IC}$  (E813) measurements. Therefore, it is impossible to measure valid  $J_{IC}$  from very small specimen directly.

Consequently, a number of effort have been made to develop test techniques to extract fracture toughness from miniatured specimens[1-2]. For example, a round compact tension specimen as small as 1.38mm diameter x 2.5mm thick was used for  $J_{IC}$  measurement [1]. However, the specimen size is still too large for most irradiation capsules, particularly in fusion program. Therefore, it is essential to determine fracture toughness from still smaller specimens.

In the present investigation, in order to develop a procedure of fracture toughness determination from small specimen such studies were considered necessary: (1) to demonstrate size effect on fracture toughness, (2) to investigate fracture modes in small specimen and (3) to analyze the relation between valid fracture toughness  $J_{Ic}$  and global toughness  $J_{in}$  and finally to predict valid fracture toughness  $J_{Ic}$  from data for invalid size specimen (0.2TCT, 0.5mm thick).

## 2. Experimental Procedure

The materials used for the present investigation were martensitic stainless steel HT-9 and nuclear pressure vessel steel A533B-1. The chemical composition and mechanical properties at room temperature are given by Table 1 and 2.

Table 1 --Chemical composition (weight percent)

Material	C	Si	Mn	P	S	Ni	Cr	Mo	V	Cu	N
HT-9	0.2	0.21	0.52	0.008	0.01	0.52	12.24	1.003	0.29	...	0.063
A533B-1	0.17	0.20	1.48	0.011	0.006	0.58	0.16	0.520	0.003	0.13	...

Table 2 --Mechanical properties at room temperature.

Materials	MPa	MPa
HT-9	725	896
A533B-1	495	620

Compact tension specimens of 25, 10, 3, 0.5mm thickness were prepared as shown in Fig.1. All of specimens are found to satisfy the minimum thickness requirements of ASTM (E813), except the 0.5mm thick specimen of HT-9 and the 3 and 0.5mm thick specimens of A533B-1. 0.5mm thick specimens were sliced from 5mm thick specimen with fatigue precracked.

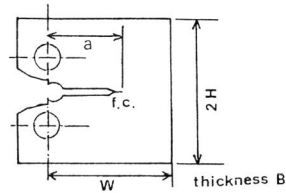


FIG.1---Specimen geometries and dimensions.

After fatigue cracking, the specimens were loaded monotonically to various displacement levels at room temperature, which correspond to different levels of crack extension. Then specimens were unloaded and heated to 400°C for half an hour to heat tint the cracked area. Crack length  $\Delta a$  (average value of nine points from front to back surface) was measured optically. Some of the unloaded A533B-1 specimens were heated for 3h at 700C in vacuum for recrystallization annealing[3]. Around the crack tip, the original bainitic microstructure changed to ferritic in the region where the equivalent plastic strain attained >20%. Photographs of recrystallized grains were

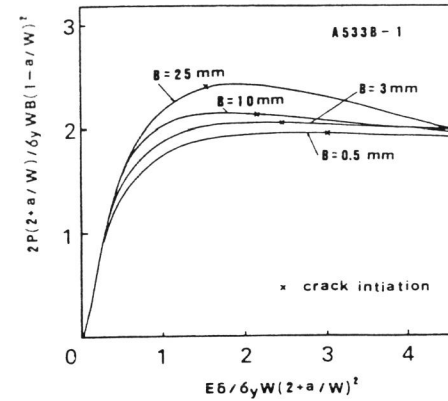


FIG.2--Normalized load vs load-line displacement curve for HT-9.

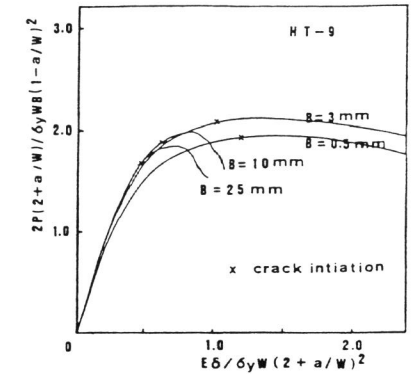


FIG.3--Normalized load vs load-line displacement curve for A533B-1.

taken by optical microscopy with 100 x magnification, from which the grain size was measured. Plastic work  $W_p$  was calculated from the expression (3).

$$W_p = \sum_{i=1}^n w_i S_i \quad (1)$$

$$w = \int \sigma d\epsilon_p$$

where  $w$ : density of plastic work,  $S$ : recrystallized area,

$\sigma$ : equivalent stress,  $\epsilon_p$ : equivalent strain

The equivalent stress was determined experimentally in a uniaxial tensile test as a function of equivalent plastic strain.

The values of  $J$  were calculated from the Merkle-Corten relationship:

$$J = (A/Bb)f(a/W) \quad (2)$$

where  $A$  is the area under the load vs load-line displacement curve,  $B$  is the specimen thickness,  $b$  is the initial uncracked ligament,  $a$  is crack length and  $f(a/W)$  is a dimensionless coefficient value. For the valid size specimen,  $J_{Ic}$  was determined by the value of the intersection of the blunting line ( $J = 2\delta\Delta a$ ) and  $J$  vs  $\Delta a$  curve. For invalid size specimen, the blunting line used is the actual blunting line.

## 3. Experimental Results

The experimental results of this study will be considered in the following sequence. First the  $J_{Ic}$  ( $J_{in}$ ) data from test on HT-9 and A533B-1 are presented for the various specimen thickness. Second, the through-thickness distribution  $W_p$  of the intense strain region at the section normal to plane surface and crack plane are presented. Third, the distribution of stretched zone width along the thickness and SEM fractograph characterizing slant fracture and flat fracture are presented. Fourth, these results are combined with rigid plastic analysis to predict valid fracture toughness.

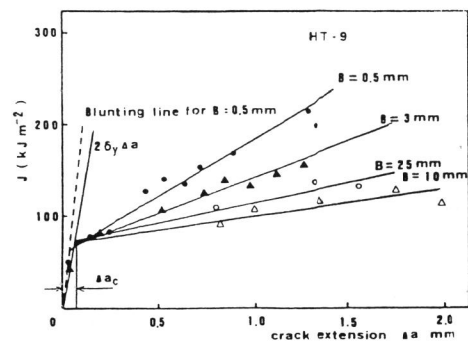


FIG. 4--J-R curves for 25, 10, 3, 0.5mm thick specimens of HT-9.

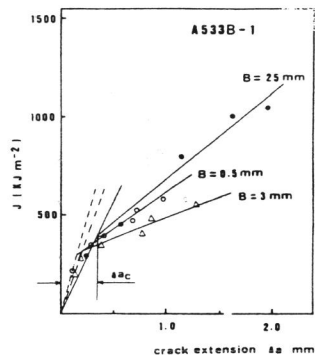


FIG. 5--J-R curve for 25, 3 0.5mm thick specimen of A533B-1.



FIG. 6--Through-thickness distribution of intense strain region at section normal to plane surface and crack plane.

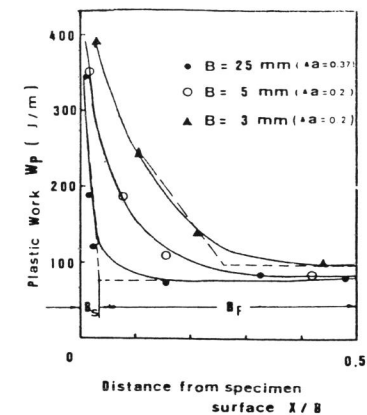


FIG. 7--Distribution of plastic energy dissipation  $W_p$  along specimen thickness.

### 3.1 J- $\Delta a$ curve

The normalized load vs load line displacement curves for various thickness specimens are shown in Figs. 2 and 3. Figure 4 and 5 show the J-R curve diagram for specimens with three different thicknesses of HT-9 and A533B-1. The actual blunting line for thin specimen is steeper than the standard blunting relationship  $J = 26\gamma\Delta a$ . This is consistent with a decrease in stretched zone size as the thickness of specimen is reduced, as discussed later. The  $J_{rc}(J_{in})$  value obtained by extrapolation using a least square fit line to the blunting line decreases as the specimen thickness decreases.

### 3.2 $W_p$ Analysis (A533B-1)

The difference between a local toughness and a global toughness is attributable to the thickness effect or the shear lip formation effect. Reflecting the stress state (plane stress at the specimen surface and plane strain at the specimen midsection), the through-thickness distribution of the intense strain region is quite characteristic. This characteristic distribution of the intense strain region can be displayed with photographs at sections normal to the plate surface and the crack plane. The result is shown in Fig. 6. The formation of the shear lip is directly affected where the intense strain region formed near the specimen surface. By measuring recrystallized grain size, equivalent plastic strain was determined [4]. From equation (1), plastic energy  $W_p$  can be obtained. Figure 7 shows the distribution of plastic energy dissipation  $W_p$  within the intense strain region at crack tip along specimen thickness of 25, 5, 3 mm.  $X$  is the thickness coordinate from specimen surface.

### 3.3 Fractographic Observation

The stretched zone boundaries were determined by high magnification scanning electron micrographs. The distributions of stretched zone width along the

thickness coordinate shown in Fig. 8(a), (b), indicates that the stretched zone near the specimen surface where shear deformation occurred is very small and the stretched zone near the surface in the thin specimen is smaller than that in the thick specimen, where  $S_{max}$  is the maximum stretched zone at the midthickness of specimen. From this observation, it is clearly understood that the shear deformation suppresses the formation of stretched zone. Thus, the standard blunting line ( $J = 26\gamma\Delta a$ ) should not be used in a very thin specimen.

As can be seen from Fig. 9(a) the overall fracture mode of 0.5mm thick specimen indicates ductile rupture. However, the feature of dimple fracture in the center region of specimen are much different from those in the two edge region. Shear dimples can be found in Fig. 9(b) from matching fractographs of microvoid [5]. Figure 9(c) shows large dimples in the center region of specimen, where those dimple are equiaxed dimple by matching and larger than those near the specimen surface. It is because the constraint to through-thickness deformation due to a triaxial stress state is a maximum at the center of the initial crack front. A study of higher magnification SEM fractographs indicates that the crack extension region can be primarily divided into two fracture modes; the shear fracture region  $B_s$  near specimen surface corresponding to mode III and the flat fracture region  $B_f$  in the center region corresponding to mode I. Thus fracture in small specimens was dominated by mixed mode I and III.

### 3.4 Prediction of Valid Fracture Toughness $J_{rc}$ from Thin Specimen Data

Through-thickness distribution of plastic energy dissipation within the intense region and the fracture mode observations using SEM suggest that the shear fracture region  $B_s$  and the flat fracture region  $B_f$  can be divided even in small specimen. The local toughness in the center region  $B_f$  of the small specimen could be used to predict a global toughness for a valid size specimen because the fracture deformation mechanism in plane strain region  $B_f$  is considered to be the same as that of large specimen. In this prediction,

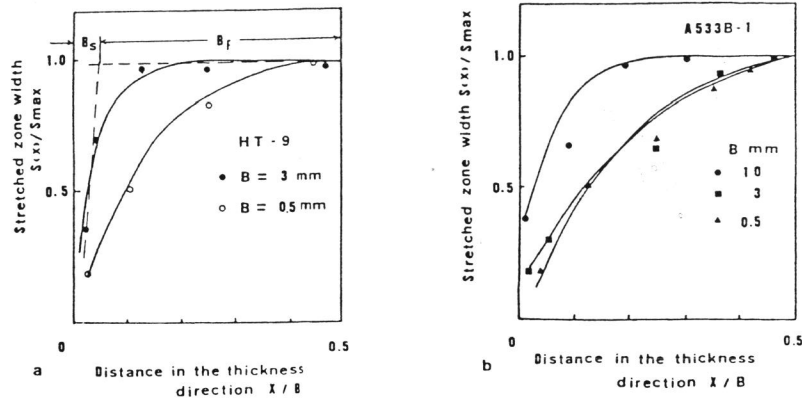


FIG.8--Distributions of normalized stretched zone width along the thickness coordinate: (a)HT-9, (b)A533B-1.

the assumption has been made that plane strain and plane stress conditions prevail in the flat and shear fracture regions respectively. Using rigid plastic analysis to I-III mixed mode fractured specimen [6], the relation between the value of J integral for the plane strain condition and the global J integral value for a mixed fracture specimen is given by [6]

$$J_{\text{plain strain}} = J_{\text{global}} / (1 - (1 - 1/\beta)(2B_s/B)) \quad (3)$$

where  $\beta$  is plastic constraint factor, (if  $a/W = 0.5$  and  $0.6$ ,  $\beta = 1.593$  and  $1.559$  respectively [6], and  $B_s$  is the thickness in plane stress condition. If  $B_s$  is considered as the thickness for a plane stress condition at ductile crack initiation, then from Eq (3), the plain strain condition  $J_{IC}$  can be expressed by global  $J_{in}$  for the mixed mode fracture specimen at crack initiation as follows:

$$J_{IC} = J_{in_{\text{global}}} / (1 - (1 - 1/\beta)(2B_s^*/B)) \quad (4)$$

The crack length  $\Delta a$  at crack initiation for different thickness specimens is obtained from Fig.4 and 5. Then, through-thickness distributions of plastic work at section normal to plane surface and crack plane obtained at section  $\Delta a = \Delta a_c$  from original crack tip are divided into two regions  $B_s$  and  $B_f$  as shown in Fig.7,8. The data of  $B_s$  from recrystallization, shear fracture and stretched zone observation for various thickness specimen is listed in Table 3. Substituting the shear fracture region thickness  $B_s$  at crack initiation to Eq(4), the fracture toughness  $J_{IC}$  was obtained as shown in table 3. Figure 10 shows the predicted  $J_{IC}$  from both recrystallization results and fractographic observations for various specimens of HT-9 and A533B-1 are in good agreement with the toughness  $J_{IC}$  obtained from valid size specimen (e.g. 1CT).

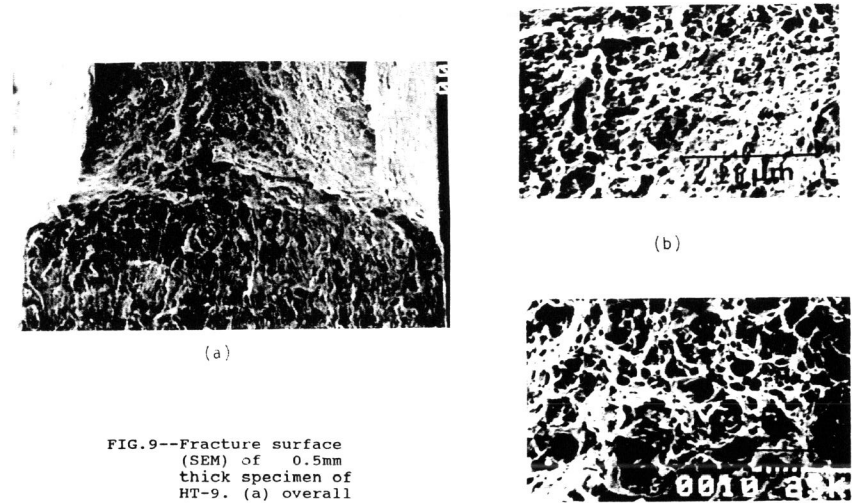


FIG.9--Fracture surface (SEM) of 0.5mm thick specimen of HT-9. (a) overall fracture, (b) shear fracture near specimen surface, (c) large dimples at the specimen center.

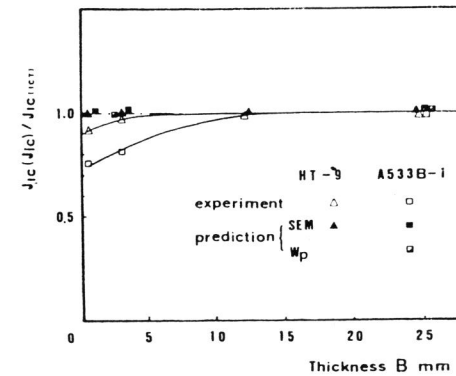


FIG.10--Change in dimensionless fracture toughness  $J_{IC}(J_{in})$  with specimen thickness and comparison of predicted J from rigid plastic analysis and valid J from 1CT specimens.

Table 3 --Predicted  $J_{Ic}$  by rigid plastic analysis, recrystallization method and fractographic observation.

Material	Size	B, mm	$J_m$ , KJ/m <sup>2</sup>	$\Delta a_0^{++}$ , mm	$2B^*/B$ (SEM)	$2B^*/B$ ( $W_p$ )	Predicted $J_{Ic}$ by Eq. 4-	
							SEM	$W_p$
HT-9	1T	25	70*	0.05	0.05	...	71.3	...
	0.4T	10	69*	0.05	0.08	...	71.1	...
	0.2T	3	67*	0.05	0.13	...	70.4	...
	0.2T	0.5	64*	0.04	0.32	...	70.9	...
A533B-1	1T	25	400*	0.37	0.08	0.04	412	406
	0.2T	3	320	0.20	0.6	0.55	412	402
	0.2T	0.5	300	0.15	0.75	...	416	...

+ from valid size specimen  
 ++ crack length at crack initiation determined by the blunting line and the crack resistance curve

#### 4 Conclusion

1. Fracture toughness  $J_{Ic}$  ( $J_{Ic}$ ) is dependent on specimen thickness and decreases slowly as the specimen thickness is reduced.
2. The crack extension for thin specimens of HT-9 and A533B-1 steels is via a I-III mixed mode fracture, which is flat fracture in the center region of specimen and shear fracture near the specimen surface.
3. The stretched zone size decreases near the specimen surface. Shear fracture deformation produced no stretched zone.
4. By using rigid plastic analysis and shear fracture measurements with the recrystallization method and fractographic observation, valid fracture toughness  $J_{Ic}$  has been predicted from a miniaturized specimen (0.2CT, 0.5mm thick).

#### 5 REFERENCES

- [1] Huang, F.H. and Gelles, D.S., "Influence of Specimen Size and Microstructure on the Fracture Toughness of a Martensitic Stainless Steel", Engineering Fracture Mechanics, Vol.19, No.1, 1984, pp.1-20.
- [2] Lucas, G.E., Shekherd, J.W., Odette, G.R., Monnell, P. and Prinn, J., "Subsized Bend and Charpy-V-notch Specimen for Irradiated Material Testing", ASTM STP 888, 1986, pp.305.
- [3] Shoji, T., Takahashi, H., and Suzuki, M., "Significance of Crack Opening Displacement and Crack Tip Plastic Strain Energy in Fracture Initiation", Metal Science, Vol.12, 1978, pp.579.
- [4] Shoji, T., "Crack Tip Blunting and Crack-Opening Displacement under Large Scale Yielding" Metal Science, Vol.5, 1976, pp.165.
- [5] Beachem, C.D., Fracture Vol.1, Ed. H. Liebowitz, Academic Press, 1968, pp.244.
- [6] Miyoshi, T., Shiratori, M. and Nemoto, M., "Discussing about Specimen Thickness Effect on J-integral", Journal of the Japan Society of Mechanical Engineers, Vol.48, No.425-436, 1982, pp.1136. (in Japanese)